ISSN: 2573-962X

Research Article

Journal of Pharmaceutical Research

Apriori Prediction of Patient Outcomes: Clinical Translation of Efficacy of An Antibody Drug Conjugate to Human

Renu Singh[1*] and Patrice Bouchard[2]

[1]*DMPK, Early Development, Aurigene Oncology Ltd*

[2]*Biologics, Human Health Therapeutics Research Centre, National Research Council Canada, Montreal, Quebec, H4P 2R2, Canada*

[*]Corresponding Author
Renu Singh, DMPK, Early Development, Aurigene Oncology Ltd.

Submitted: 2024, Mar 25; **Accepted:** 2024, Apr 25; **Published:** 2024, Apr 30

Citation: Singh, R., Bouchard, P. (2024). Apriori Prediction of Patient Outcomes: Clinical Translation of Efficacy of An Antibody Drug Conjugate to Human. *J Pharmaceut Res, 9*(1). 01-11.

Abstract

Translation of preclinical efficacy of an antibody drug conjugate (ADC) was done to determine dose and dosing regimen for first in human (FIH) study by simulating clinical trial in virtual cancer patients. Clinical trial simulations were done in 50 virtual subjects, systems parameters of PK/PD model were adapted to NSCLC patients for these simulations. It was found that at doses above 1.6 mg/kg Q1W, steady state trough concentrations (Ctrough-ss) were above TSC. The predicted progression free survival (PFS) was approximately 55, 72 and 85% at doses of 0.5, 1 and 2 mg/kg Q1W, while at doses of 1.3, 2.6 and 3.9 mg/kg Q3W survival was predicted to be 50, 65, 80%. Clinical efficacy at high doses and less frequent dosing, wherein average steady state concentrations of conjugated antibody are maintained above TSC was similar to that obtained by maintaining Ctrough-ss at TSC at low dose and more frequent dosing regimen. Therefore, maintaining Ctroughss above the TSC may not be required for improving PFS. A human dose which maintains average steady state concentrations at predicted TSC is sufficient to obtain clinical efficacy and therefore maintaining steady state trough concentrations above TSC may not be desired.

Keywords: Virtual Clinical Trial, Anti-body Drug Conjugate, Modelling and Simulation, Translation, Efficacy, Cancer

1. Introduction

Antibody drug conjugate (ADCs) are one of the modalities that hold significant promise in improving therapeutic outcome in cancer patients. Their unique ability to deliver a molecule to the target cell makes them standout as a modality compared to small molecule or antibodies. However, complexities in the optimization of their key attributes as well as challenges in understanding efficacy-toxicity window has led several pharmaceutical companies to abandon their development [1]. Nevertheless, recent approval of six more ADCs has revived interest in the field and has spurred evaluation of innovative approaches to develop next generation ADCs with improved efficacy and tolerability [2,3,4].

Like any other therapeutic, developing understanding of target modulation and downstream efficacy are important for ADCs because of their narrow therapeutic window [4,5]. Designing preclinical studies to establish robust exposure response is the first step in this direction. Translation of preclinical efficacy to human is a subsequent step, which needs to be supported by sound pharmacology rationale, understanding of preclinical-clinical differences and population heterogeneity [6,7,8]. These two key steps form the basis of a successful clinical outcome. PK/PD (Pharmacokinetic/Pharmacodynamic) modeling and simulation can play a pivotal role in establishing concentration-effect relationship and translation of preclinical efficacy to clinical efficacy [9,10]. In particular, its value has been seen in supporting justification for safe starting dose and relevant dose escalations for oncology and immuno-oncology therapeutics [9,11].

In addition to understanding concentration-effect relationship or threshold concentration required to see target modulation from preclinical studies, accurate translation of human pharmacokinetics from preclinical data is also very important for effective preclinical to clinical translation [8]. Variability in pharmacokinetics of a therapeutic candidate in patient population is an important factor which is often neglected in first-in-human (FIH) dose selection. Evaluating inter-subject variability in drug pharmacokinetics and pharmacodynamics helps to ensure that all patients attain suitable drug exposure to achieve efficacy or avoid toxicity. Population modelling is a useful tool to identify important covariates that effect pharmacokinetics thus aiding in the understanding factors contributing to inter-subject variability (12). Based on prior information or experiences, this evaluation can be employed early in drug discovery setting to predict human pharmacokinetic prior to clinical trials [13,14]. Combining predicted human PK variability with apriori

prediction of clinical efficacy can serve as a powerful tool for not only selecting appropriate dosing regimen but also efficacious dose for FIH studies.

We have translated preclinical efficacy of an ADC to human using PK/PD modelling and simulation to define human dose and regimen for FIH study. ADC evaluated is chimeric monoclonal antibody conjugated to payload using a non-cleavable linker. Preclinical efficacy of ADC was evaluated in H292 xenograft SCID mice at various dose levels (1.5 to 15 mg/kg). Blood samples were collected from mice by staggered sampling such that samples were collected from all mice. Data of H292 efficacy study was used to build the PK/PD relationship of ADC in mice using tumor growth inhibition model to enable estimation of tumoristatic concentration (TSC). The pharmacokinetics of ADC was also characterized in cynomolgus monkey. Cynomolgus monkey concentration-time data was scaled to human using species time-invariant method to estimate human pharmacokinetic parameters. Population PK/PD modelling was done to capture inter-animal variability in the efficacy of ADC. Inter-subject variability in pharmacokinetic of total and conjugated antibody in human was also incorporated during simulation of human pharmacokinetic profile using body weight as a covariate as well as by using residual variability in scaled pharmacokinetic parameters. Tumor regression was predicted in 50 patients using a population clinical PK/PD model, wherein tumor growth inhibition parameters determined from PK/PD modelling of xenograft mice were used, while systemic specific parameters were modified to represent NSCLC (non-small cell lung cancer) patient population. Progression free survival (PFS) was determined at various clinical doses and regimens to establish whether predicted efficacious dose and regimen could produce desired clinical outcome.

2. Materials and Method

2.1. H292 Xenograft Study

The study was conducted at University of Western Ontario (UWO) and was approved by local Institutional Animal Care and Use Committee (IACUC). All the animal studies were conducted after the approval of the study protocol by UWO animal ethics and IACUC. Briefly, male SCID mice were randomized apriori into groups of 4 mice per treatment group. H292 NSCLC cells (ATCC, Manassas, VA) were injected into both the right and left flanks of each mouse (6 X 10^6 cells per injection site) and allowed to grow into tumors of 100 mm^3. When tumors in each mouse reach the desired volume (100 mm^3), each mouse was injected with the planned treatment agent (Day 0). The test article was administered i.p. at dose levels of 1.5, 3.0, 7.5 and 15 mg/kg on days 0, 7, 11, 15 and 19 which correspond to cycles 1, 2, 3, 4 and 5. Blood samples were collected by staggered sampling to alternate the blood collection at each time-point (n= 1/time point/group). Samples were collected at 0.25, 2, 24, 48, 72, 120 and 168 h post-dose in cycle 1 and cycle 5; at 0, 2, 24 and 120 h post-dose in cycle 3 and at 0.25, 48, 72 and 168 h post-dose in cycle 4.

Blood samples were processed to serum and analyzed for the quantitation of total antibody, conjugated antibody and free payload. Caliper measurements were done for estimating tumor volumes. Tumor volumes were measured on days 0, 7, 11, 14, 18, 21, 25, 30, 37, 44, 51 and 57 and the percent of the volume for each tumor was calculated with respect to Day 0.

2.2. Cynomolgus Monkey Study

The study was conducted at University of Western Ontario (UWO) and was approved by local Institutional Animal Care and Use Committee (IACUC). All the animal studies were conducted after the approval of the study protocol by UWO animal ethics and IACUC. ADC was administered via one-hour intravenous infusion once weekly for 4 weeks to cynomolgus monkeys at 10 or 20 mg/kg. Blood was collected pre-infusion, 1, 3, 6, 9, 24, 72, 120 and 168 h post-infusion and was processed to serum. Processed samples were used for measuring serum concentration of total and conjugated antibody, free payload and anti-ADC antibodies.

3. Bioanalysis

3.1. Total Antibody and Conjugated Antibody

Mice and monkey serum samples were diluted appropriately with PBS containing 1% BSA. Diluted samples were loaded onto ELISA plates were coated with target antigen for total antibody assay. ELISA plates coated with anti-payload mouse antibody were used for detection of conjugated antibody. Goat anti-human IgG AP (Jackson Immuno) was used as a secondary antibody for both assays. The signals were developed with para-nitrophenylphosphate and absorbance was measured at 405 nm (Envision plate Reader, Perkin Elmer Inc., Waltham, Massachusetts). Standard curves with 5PL fitting and interpolation of unknown samples were analyzed using Envision software (Perkin Elmer Inc., Waltham, Massachusetts).

3.2. Pharmacokinetic Data Analysis

Pharmacokinetic parameters were estimated using Phoenix NLME 8.0 (Certara, St. Louis, Missouri, USA). The nominal dose administered to each dose group was determined by NanoDrop spectrophotometer (Thermo Fisher Scientific, Waltham, Massachusetts) and was used for pharmacokinetic analysis. A two-compartment model was used to fit total and conjugated antibody serum concentration data. Population estimates for absorption rate constant (Ka), clearance (CL, CL2), and volume (V, V2) were used for subsequent PK/PD modeling of tumor regression data.

3.3. Estimation of TSC in H292 Xenograft Mice

A tumor growth inhibition model was used to describe antitumor activity of ADC in H292 xenograft mice using pharmacokinetic and efficacy data [15]. In this model, the population pharmacokinetic parameter estimates for K_a, CL, CL_2, V and V_2 generated from the pharmacokinetic analysis were used as initial estimates for the population PK/PD model. Since efficacy was considered to be driven by conjugated antibody, subsequent PK/PD modelling was done using concentration-time data of this analyte. A simultaneous PK and PD model-fitting was done using First-Order Conditional Estimation Extended Least Squares (FOCE ELS). Following parameters were estimated by PK/PD modelling: pharmacokinetic parameters of conjugated

antibody, pharmacodynamic parameters of net tumor growth rate in the absence of drug (K_{gro}), tumor death rate constant (K_{out}), half maximal tumor growth inhibitory concentration (IC50), hill coefficient (gamma), tumor net growth rate (K_{ng}), E is the effect and K_{max} is maximal tumor growth inhibition effect constant. TSC (tumoristatic concentration), the predicted concentration at which there is no net tumor growth was calculated using the differential equation describing tumor growth as shown in equation 6. The following equations were used for deriving the pharmacodynamics parameters:

$Inh = K_{max} * (C / (tvIC_{50} + C))$ .....Equ 1

$deriv(E1 = (K_{gro} - Inh * K_{out}) * E11^{(2/3)})$ .....Equ 2

$deriv(E2 = (Inh * K_{out} * E11^{(2/3)} - K_{out} * E21^{(2/3)}))$ .....Equ 3

$deriv(E3 = (K_{out} * E21^{(2/3)} - K_{out} * E31^{(2/3)})$ .....Equ 4

$E = E1 + E2 + E3$ .....Equ 5

$TSC=(tvK_{gro}*tvIC_{50})/(tvK_{out}*(tvK_{max}-tvK_{gro})$ .....Equ 6

3.4 Human PK Prediction

The serum concentration-time profiles of total and conjugated antibody in cynomolgus monkeys following IV infusion at 10 and 20 mg/kg were transformed to human concentration-time profiles using the species invariant time method described by Dedrick [16]. Briefly, the equivalent times were transformed from monkey data using the following equations:

$$Time_{human} = Time_{cyno} \cdot \left(\frac{\text{Body weight}_{human}}{\text{Body weight}_{cyno}}\right)^{Exponent_{volume} - Exponent_{clearance}}$$

.....Equ

The human-like concentrations were estimated using the following equation:

$$Concentration_{human} = Concentration_{cyno} \cdot \left(\frac{Dose_{human}}{Dose_{cyno}}\right) \cdot \left(\frac{\text{Body weight}_{cyno}}{\text{Body weight}_{human}}\right)^{Exponent_{volume}}$$

.....Equ 8

Wherein, $Time_{cyno}$, $concentration_{cyno,}$ $dose_{cyno}$, $body\ weight_{cyno}$ are observed time, concentration, and administered dose in cynomolgus monkeys and body weight of monkeys, respectively. $Time_{human}$, $concentration_{human}$, $body\ weight_{human}$, $dose_{human}$ are predicted human parameters. Allometric equations used scaling exponents of 0.85 for CL and 1 for V, respectively [17,18]. Since non-linearity was observed for clearance in monkeys, systemic clearance was accounted by linear and nonlinear elimination. The bi-exponential pharmacokinetic profiles estimated for human using the above equations were fit to a two compartmental model with linear and non-linear clearance from central compartment using Berkley Madonna 8.3.18 (Macey and Oster, Berkeley, CA) to estimate human pharmacokinetic parameters. Since conjugated antibody was considered as pharmacological active analyte all modelling and simulations were performed only for conjugated antibody. The estimates of V_1, V_2, Cl_1, Km and Vmax were determined by fitting predicted human profiles at 10 and 20 mg/kg. Estimated parameters served as input for simulations of serum conjugated antibody concentrations in human. Population modelling was done using non-linear mixed effects modelling in order to predict variability in human pharmacokinetics. Simulations were done in different dosing regimen scenarios in 50 healthy subjects using body weight as a covariate using Berkley Madonna 8.3.18 (Macey and Oster, Berkeley, CA).

3.4. Clinical Trial Simulations

Tumor regression was simulated in 50 patients in different dosing regimens and doses using pharmacodynamic parameters estimated from preclinical efficacy models. Two compartment model with linear and non-linear clearance from central compartment was used for pharmacokinetics and pharmacodynamic was described by Jumbe transduction model [15]. Pharmacokinetic and pharmacodynamic parameters mentioned in Tables 1 and 2 were used as estimates in population PK/PD model. Residual variability in PD model was assumed to be 30% while pharmacokinetic variability was simulated by using body weight as a covariate. Tumor growth rate represented by K_g in the PD model was changed according to tumor doubling time values reported in literature for NSCLC [19,20]. Tumor volume was simulated for 3 months in Q1W regimen and 6 months for Q3W regimen to mimic typical protocol in clinical settings. All simulations were done in Berkley Madonna 8.3.18, Macey and Oster, Berkeley, CA) and data was transformed in GraphPad Prism 7.05 (GraphPad Software Inc., San Diego, California). For each simulated clinical trial, predicted tumor volumes were determined over time and progression free survivals (PFS) were calculated. Tumor regression data was subsequently translated to obtain Kalpan-Meier curves to compare therapeutic benefit of ADC in different dose and dosing regimen scenarios. For estimating PFS, Response Evaluation Criteria in Solid Tumor (RECIST 1.1) criteria was applied [21, 22]. According to RECIST 1.1 criteria, definitions of minimum size of measurable lesion is ≥ 10 mm by CT and MRI. The criteria to categorize response rates for progressive disease, stable disease, partial regression, and complete regression for lung cancer were more than 20% increase in tumor diameter, less than 30% reduction in tumor diameter, more than 30% decrease in tumor diameter but still detectable, and below the detection limit of 10 mm tumor diameter, respectively.

4. Results

The serum-concentration profiles of conjugated antibody and of the total antibody after single i.p. administration to tumor bearing mice at different dose levels are shown in Figure 1.

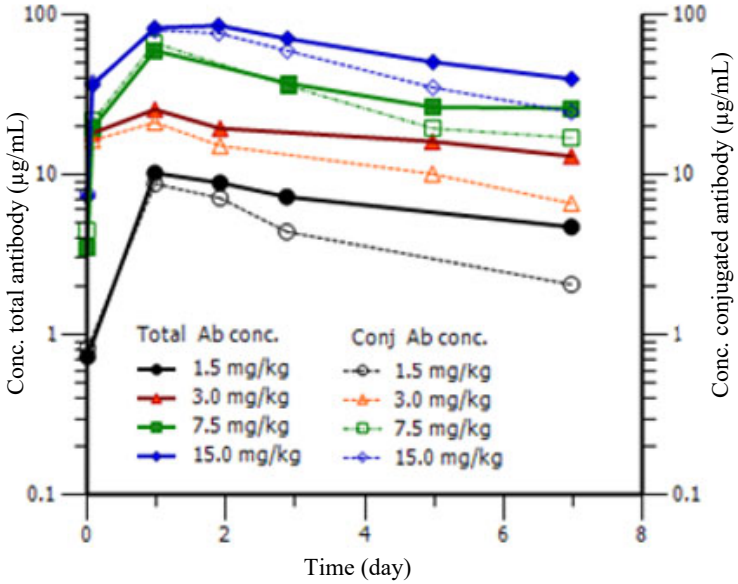

Figure 1: Serum-concentration time profiles of total antibody and conjugated antibody after i.p. administration to H292 tumor bearing SCID mice. ADC was administered by intraperitoneal injection at doses of 1.5, 3.0, 7.5 or 15 mg/kg on Days 0, 7, 11, 15 and 19. Blood samples were collected after dosing on Day 1 to measure serum concentrations of total antibody and conjugated antibody. Samples were collected by staggered sampling such that n= 3/time point/dose group.

Free payload concentrations were below LLOQ at all timepoints. Exposure of both conjugated and total antibody increased proportionally with dose. The serum-concentration profiles at all dose levels were found to fit a two-compartment model. Since blood samples were collected from different mice at different time points, PK parameters were derived by population modelling. The data from all dosing cycles was used for estimating pharmacokinetics parameters (Table 1).

Parameter	Unit	Estimate	SD
Ka	(1/day)	2.39	1.41
V	(mL/kg)	49.8	23.1
Cl	(mL/kg/day)	24.3	1.88
V_2	(mL/kg)	105	40.4
Cl_2	(mL/kg/day)	109	47.2

Table 1: Population Pharmacokinetic Parameters of ADC in H292 Xenograft Mice

Absorption rate constant (K_a) was determined to be 2.39 day^{-1}. Distribution volumes V_1 and V_2 were 49.8 and 105 mL/day, respectively. Cl_1 was 24.3 mL/kg/day and Cl_2 was estimated to be 110 mL/kg/day, respectively. Precision of was low for some of the estimated population parameters because data of all 4 cycles was taken in account for estimating pharmacokinetic parameters.

H292 cells were inoculated on both flanks of SCID mice and allowed to grow until they reached 100 mm^3. After the desired tumor size was reached, mice were randomized into different groups. Animals of control group were administered vehicle control while remaining mice were treated with ADC. The tumor volume measurements were done on days 0, 7, 11, 14, 18, 21, 25, 30, 37, 44, 51 and 57. As seen in Figure 2, tumors continued to grow well in control group while those treated with ADC showed inhibited growth. At 1.5 mg/kg tumor growth was markedly reduced compared to control group, however, high inter-animal variability was observed in tumor volumes. Complete tumor regression was observed at doses of 3, 7.5 and 15 mg/kg.

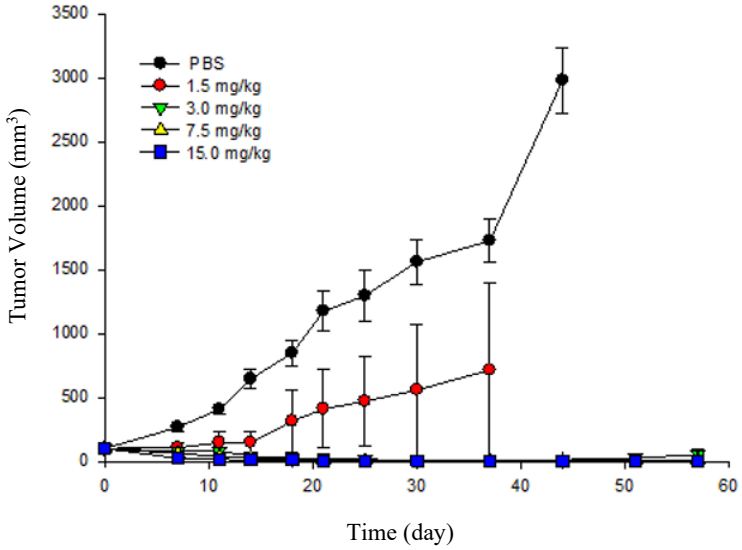

Figure 2: Repeat-Dose of ADC results in tumor reduction and elimination in a Non-Small Cancer Cell Xenograft mouse model (H292 Cells).

A tumor growth inhibition model was used to describe antitumor activity of ADC in H292 xenograft mice using pharmacokinetic data. Non-linear mixed effects modeling was used to enable population modeling of the data so that inter-animal variability in observed data could be captured and translated to human. Gamma was fixed to 1.0 based on analysis of diagnostics and maximum log likelihood. Despite high inter-individual variability in pharmacodynamic response and relatively small size of this preclinical dataset, population PK/PD model was able to capture dose-dependent efficacy of ADC reasonably well. Population pharmacodynamic parameter estimates are listed in Table 2.

Parameter	Estimate	Unit	SD
tvK_{gro}	0.88	1/day	0.07
tvK_{out}	1.59	1/day	1.78
tvK_{max}	3.49	1/day	8.48
$tvIC_{50}$	14.3	µg/mL	32.5
tvTSC	1.06	µg/mL	0.66

Table 2: Population Pharmacodynamic Parameters Obtained After Fitting Tumor Volume Data to Tumor Growth Inhibition Model

Estimated values of K_{gro}, K_{out} and K_{max} were 0.88, 1.59, 3.49 day^{-1}, respectively. In vivo IC_{50} of conjugated antibody was determined to be 14.3 µg/mL. TSC was determined to be 1.06 µg/mL with 95% confidence interval ranging from 0.30 to 1.30 µg/mL. Estimated TSC of 1.06 µg/mL was considered a conservative target for achieving efficacy in clinical setting. For the purpose of predicting human concentrations of ADC, data obtained from toxicology study conducted in cynomolgus monkey was leveraged. Serum samples from this study were analyzed for conjugated antibody, total antibody and free payload. Free payload concentrations were measurable only for first few timepoints postdosing and were not used for any subsequent analysis. Terminal half-life of conjugated antibody was shorter than that of total antibody with values of 30 h for conjugated antibody and 34.7 h for total antibody at 10 mg/kg. At 20 mg/kg, terminal half-lives were estimated to be 48.5 and 62.3 h for conjugated and total antibody, respectively (Supplementary Information). Average total systemic clearance as determined by non-compartmental analysis in cycle 1 at 10 mg/kg was approximately 1.44 and 1.16 mL/h/kg for conjugated and total antibody. Clearance was found to decrease to 1.01 and 0.93 mL/h/kg (conjugated and total antibody) with increase in dose to 20 mg/kg. Volume of distribution at steady state was between 53.6 and 50.9 mL/kg (conjugated and total antibody) at 10 mg/kg and 53.6 and 65.2 mL/kg (conjugated and total antibody) at 20 mg/kg and suggesting ADC was primarily distributed in the central compartment. Serum concentration data of both conjugated and total antibody in cynomolgus monkey were scaled to human using species time-invariant method as mentioned in the method section. The transformed concentration data is shown in Figure 6. Evidence of non-linear pharmacokinetics of conjugated as well as total antibody was evident from change in clearance of both analytes with change in dose. With this prior information, 2-compartment model with linear and non-linear clearance from the central compartment was used to capture non-linearity in scaled human concentration time data. The estimated human parameters are listed in Table 3.

Parameter	Estimate	Unit	SD
Cl1	48.4	mL/day	1.34
V1	154	mL /kg	3.11
V_{max}	2347	mL/day	42.5
K_m	1.23	□g/mL	0.71
Cl_2	84.6	mL/day	17.0
V_2	270	mL	10.5

Table 3: Estimated Values of Clearance Saturation Model Used for Simulation.

Linear clearance (Cl_1) and distribution clearance (Cl_2) values were determined to be 48.3 and 84.6 mL/day. Population estimates for volumes, V_1 and V_2 were 154 and 271 mL. K_m and V_{max}, parameters describing non-linear clearance from the central compartment obtained from model fit were 1.23 µg/mL and 2347 mL/day. Human PK simulations were done using TSC as a target concentration required to achieve clinical efficacy. Two different scenarios were considered 1) average steady concentrations (C_{avg-ss}) are maintained at population mean TSC 2) $C_{trough-ss}$ concentrations are above population TSC. As seen in Figure 6 at dose of 0.5 mg/kg, steady state concentrations were approximately at mean TSC. At the doses of 1.6 and 2.6 mg/kg Q1W, C_{trough} concentrations stayed above mean TSC or above confidence interval of TSC. In Q3W dosing regimen, C_{trough} concentrations could not be maintained above population mean TSC at dose levels upto 3.9 mg/kg. At doses greater than 4 mg/kg safety multiples could not be maintained (data not shown), therefore simulations were not conducted at doses greater than 3.9 mg/kg Q3W. Clinical trial simulations were done in 50 subjects using information translated from preclinical PK/PD modelling and cynomolgus monkey pharmacokinetic data. Most of pharmacodynamic parameters used in the clinical PK/PD model were borrowed from preclinical model, however, to provide clinical relevance and predict efficacy of ADC in cancer patients, tumor growth rate and initial tumor volume were changed to the values reported clinically [19, 20]. PFS was determined from simulated cancer growth curves using RECIST 1.1 criteria. Population mean PFS at doses of 0.5, 1 and 2 mg/kg Q1W was approximately 55, 72 and 85 % (Figure 7). At doses of 1.3, 2.6 and 3.9 mg/kg Q3W survival was 50, 65, 80% (Figure 7).

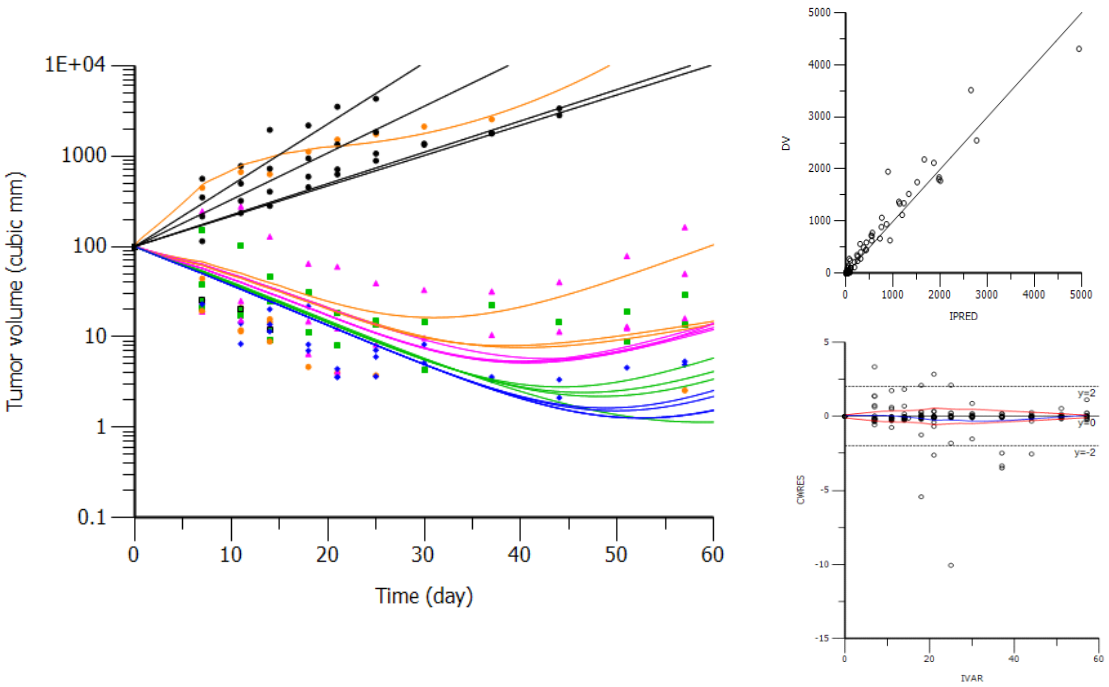

Figure 3: (a) Tumor volume PK/PD model fit for H292 xenograft tumor response to following intraperitoneal dosing of vehicle (black) or ADC dosed once on days 0, 7, 11, 15 and 19 at 1.5 mg/kg (orange), 3 mg/kg (magenta), 7.5 mg/kg (green) or 15 mg/kg (blue). Solid lines represent predicted data while data points are observed data. (b) Goodness of fit diagnostic plots: individual prediction (IPRED) versus DV and corrected weighted residual (CWRES) versus IVAR. Prediction were scattered on the line of unity suggesting very good correlation between observed and predicted tumor volume regression. CWRES were scattered mostly within 2-fold error, there was no change in weighted residuals as function of independent variable (time).

5. Discussion

PK/PD study was conducted in H292 xenograft mice in order to predict exposure response of our ADC in NSCLC cancer patients. Mice were administered doses ranging from 1.5 to 15 mg/kg and blood samples were collected from all mice in a staggered manner so that there is sufficient data to build robust understanding of efficacy in mice. Selection of these doses was based on prior studies conducted in the same model (data not shown). As seen in Figure 1, systemic concentrations of conjugated antibody as well as total antibody increased with increase in dose. It is important to mention that concentrations of free payload were below LLOQ at all doses. No evidence of changes in clearance of either conjugated or total antibody was observed with increase in dose, suggesting linear clearance. Our antibody does not bind to mouse antigen, therefore, TMDD was not anticipated to play role in clearance of this ADC in mice.

All implanted tumors were found to regress after first dose (Figure 2). Tumor growth inhibition was even marked as the study progressed, except at 1.5 mg/kg, wherein tumors were seen to regrow after first 2 doses. At doses greater than 1.5 mg/kg, no tumor regrowth was observed even 20 days after treatment was completed. In some mice, tumor was not palpable towards the end of the study, suggesting remarkable efficacy of this ADC.

PK/PD modelling was done with tumor volume and pharmacokinetic data obtained from H292 xenograft study. Several mechanistic models have been developed and reported for PK/PD modelling of ADCs [15,23,24, 5]. Model developed by Jumbe et al., 2010 remains one of the most applied models for preclinical translation of efficacy of ADCs. This model has been successfully shown to translate preclinical efficacy of T-DM1 to clinic. Because of aforementioned reasons and ease of identifiability of modelling parameters, we have used Jumbe's model for building concentration-effect relationship and deriving TSC. Population modelling was done to capture inter-animal variability in pharmacokinetics as well as tumor growth inhibition. Reasonably good fit was observed for tumor growth inhibition at all doses as seen in tumor volume data fit and diagnostic plots (Figure 3).

All parameters were estimated with a good precision as seen in Table 2. Estimated population TSC estimate was 1.06 µg/mL (confidence interval, 0.31 to 1.30 □g/mL). Non-linearity in pharmacokinetics of ADC was evident from concentration-time profiles of both total and conjugated antibody at 10 to 20 mg/kg and corresponding change in estimated systemic clearance (Figure 4, Supplementary information).

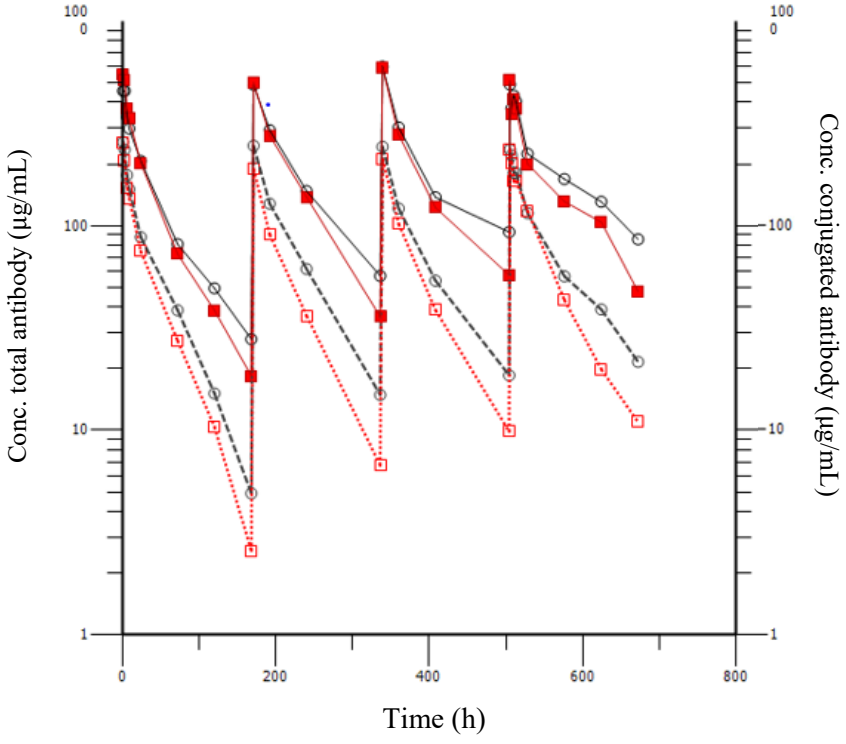

Figure 4: Serum concentration profiles of total antibody and conjugated antibody following repeated intravenous infusions of ADC to cynomolgus monkey at 10 mg/kg and 20 mg/kg. Solid lines represent data of 20 mg/kg while dash line represent data of 10 mg/kg. Circles and squares are serum concentrations of total antibody and conjugated antibody, respectively.

This non-linearity can be explained by TMDD due to binding of total and conjugated antibody to target antigen in cynomolgus monkey. Cynomolgus monkey serum concentration time data was scaled to human using species time-invariant method [16]. Allometric exponents of 0.85 and 1 were used for clearance and volume as reported previously [18]. It is important to mention that ADC binds to cynomolgus monkey and human target antigen with similar binding affinity, therefore, based on monkey pharmacokinetic data, non-linearity in pharmacokinetics ADC was also assumed in human. Two compartment model with linear and non-linear clearance from central compartment was found to fit observed serum concentration time data at both doses better than Michaelis-Menten model (data not shown). As seen in diagnostic plots (Figure 5) linear correlation was observed between observed and predicted data with most of the numbers scattered around line of unity.

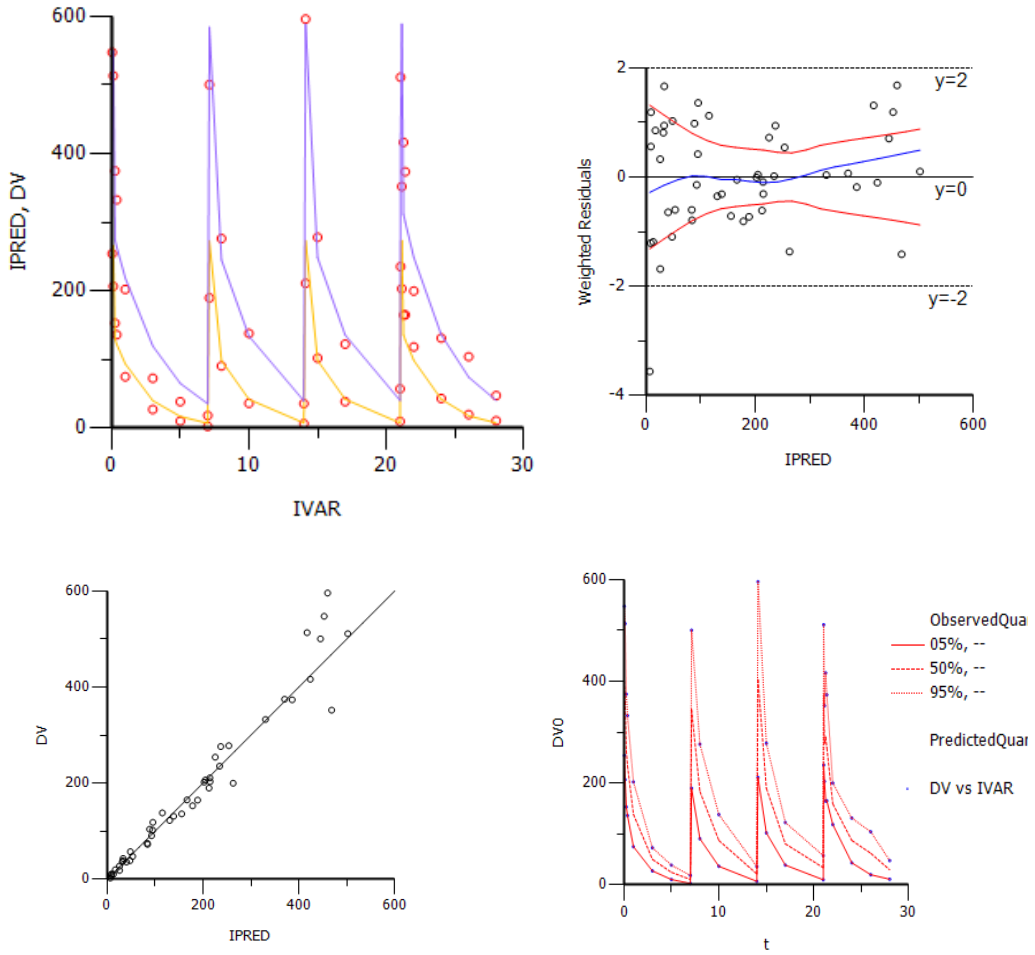

Figure 5: Model fit and diagnostic plots to demonstrate the goodness of fit the model used to fit monkey pharmacokinetics data using two compartment model with parallel and non-linear elimination from the central compartment following IV administration.

In addition, weighted residuals were within 2-fold, suggesting model fit observed concentration data very well. A closer examination of visual predicted check plots further revealed that quantiles of observed data fell within predicted quantiles corroborating goodness of the fit of the model. Human pharmacokinetic parameters: Cl_1, Cl_2, V_1, V_2, K_m and V_{max} derived from scaled pharmacokinetic data were used for subsequent simulations. Population average TSC was used as a target translation parameter driving clinical efficacy. Simulations were performed in 50 virtual individuals at doses between 0.2 to 2 mg/kg Q1W and 1 to 4 mg/kg Q3W to keep $C_{avg\text{-}ss}$ at population TSC estimate or $C_{trough\text{-}ss}$ above the TSC. Simulated profiles are shown in Figure 6.

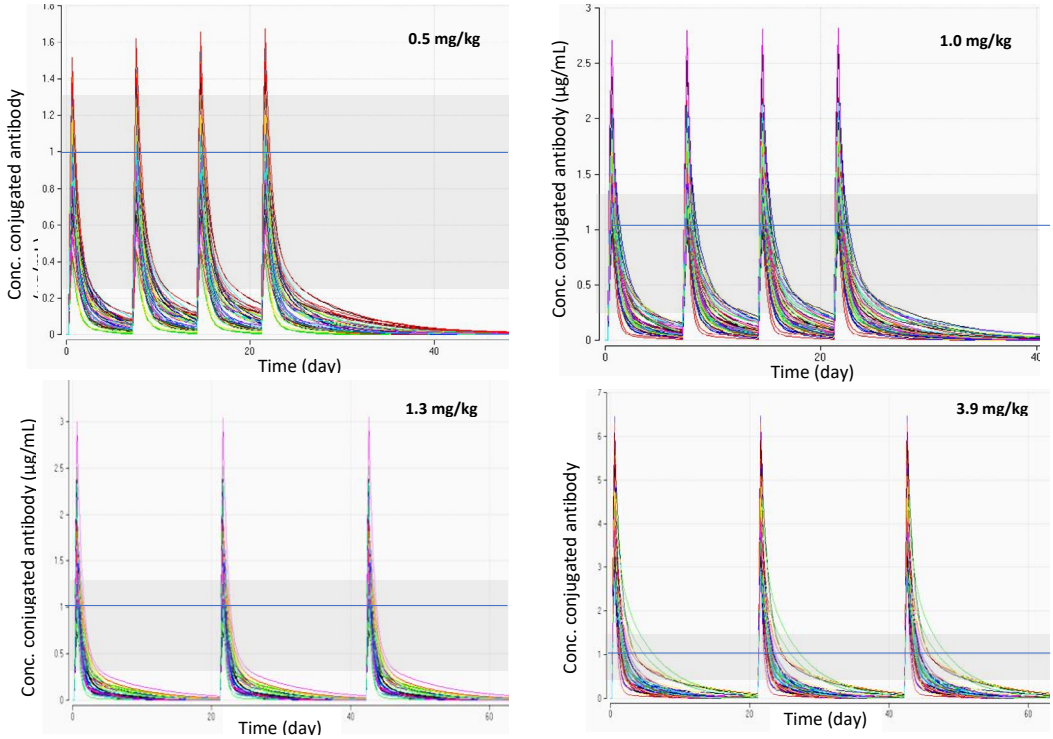

Figure 6: Simulated concentration-time profile of ADC in human at the doses of 0.5 mg/kg and 1.0 mg/kg once every week and at 1.3 mg/kg and 3.9 mg/kg once every three week for six weeks. TSC was estimated to be 1.7 µg/mL from PK/PD modelling of tumor regression data obtained form H292 xenograft mice. Concentration range in grey represents the 95% confidence interval of TSC estimate.

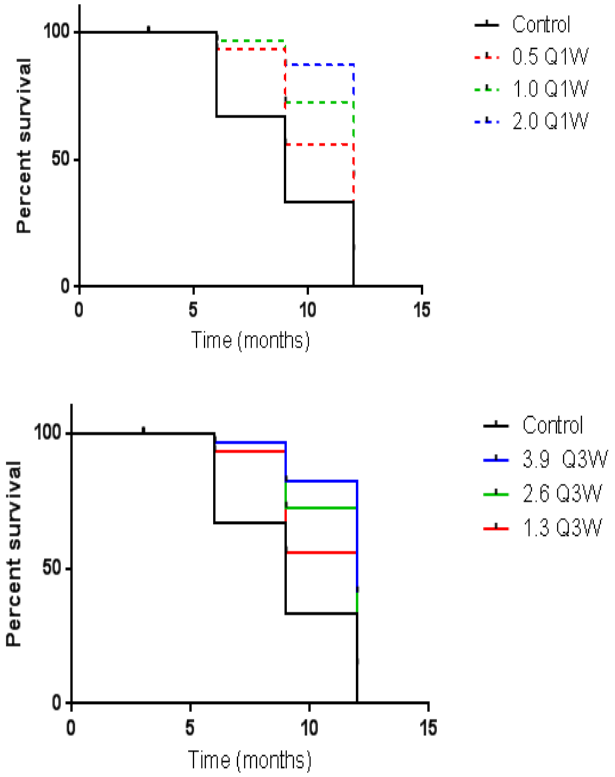

Figure 7: Kaplan Meier survival analysis of simulated therapeutic benefit of ADC in human at the doses of 0.5 -2 mg/kg and 1.3-3.9 mg/kg once every week or once every three weeks for a total of 14 or 7 doses, respectively. The tumor regression produced in clinic was simulated in 50 patients using Jumbe transduction model. For estimating patient survival tumor diameter less than 1.5 cm was assumed an arbitrary measure of survival.

Minimum systemic concentrations were found to vary about 25-30% in the simulated population, however a reasonable coverage of estimated TSC was observed (Figure 6). Population average steady state concentrations remained within estimated 95% confidence interval of TSC for doses greater than 0.5 mg/kg Q1W and 1.3 mg/kg Q3W for all simulated individuals. Our simulations showed that at dose of 1.6 mg/kg, concentrations of all simulated individuals were above 1.06 ug/mL. However, in Q3W regimen, trough concentrations could not be maintained above TSC in the simulated dose range.

In order to further understand whether maintaining systemic exposure above TSC could translate into desired therapeutic benefit in human, clinical trial simulations were conducted using pharmacodynamic parameters estimated from preclinical efficacy models. Premise of this modelling work was based on promising results shown by clinical trial for brentuximab-vedotin in Hodgkin's lymphoma, where a mechanistic mathematical model was successfully able to predict clinical efficacy of this ADC [25]. Several other successful retrospective predictions of PFS have been reported by Betts, Singh and Shah [26,27]. We have kept overall model structure for clinical trial simulation the same as preclinical model, with the exception that mouse system parameters such as initial tumor size and tumor growth rates were replaced with clinically relevant parameters, to make the model representative of the human system. Initial tumor size and tumor doubling time reported in literature for NSCLC patients were used [19, 20]. Subjects were dosed for 3 months in Q1W regimen and 6 months for Q3W regimen to mimic typical protocol in clinical settings. As seen in Kalpan Meier curves, at doses of 0.5, 1 and 2 mg/kg Q1W mean PFS was approximately 55, 72 and 85%. Similarly, at doses of 1.3, 2.6 and 3.9 mg/kg Q3W survival was 50, 65, 80% (Figure 7). This suggests, markedly similar therapeutic outcome when ADC was administered once weekly at doses between 0.5-2.0 mg/kg or once every three weeks at doses between 1.3 to 3.9 mg/kg for 3 or 6 months. Betts et al., [26]. Have used a multiscale PK/PD model to translate preclinical efficacy of inotuzumab ozogamicin and found fractionated dosing regimen was superior to a conventional dosing regimen for acute lymphocytic leukemia but not for non-Hodgkin's lymphoma. In a similar effort, Singh and Shah [27]. Compared PFS for HER2 1+ and 3+ populations in doses ranging from 0.1 to 20 mg/kg Q3W, 3.6 mg/kg Q4W, 1.2 mg/kg Q1W and 3, 0.3, and 0.3 mg/kg given on days 0, 7, and 14 of a 21-day cycle (frontloading regimen). They reported similar PFS irrespective of dosing regimen in HER2 1+, however, fractionated dosing regimen (i.e. front loading) was found to provide an improvement in the efficacy. Jumbe et al., 2010 [15]. Have also evaluated different dosing regimens for T-DM1 (Q1W, Q2W, and Q3W) in preclinical HER2-expressing animal models (BT474EEI and F05). They found lack of improvement in the efficacy of ADC when a fractionated dosing regimen was used. Similar findings were observed in clinical outcome for T-DM1 as reported by Wang et al., [28]. Wherein clinical efficacy was observed at doses where C_{min} was below preclinical estimated TSC of 30.2 µg/mL. Our findings suggest, maintaining trough concentrations above target TSC does not provide marked therapeutic benefit over maintaining average steady state concentrations of ADC at TSC. In our work, no marked improvement in PFS was noted with more frequent dosing and clinical outcome was predicted to be between Q1W and Q3W regimens. High dose of ADC wherein steady state trough concentrations is above TSC did not translate to marked clinical PFS. This finding is significant for researchers developing ADCs and optimizing clinical dose as they will not have to necessarily conduct clinical trial at high doses to maintain concentrations above TSC. Considering the challenges in understanding efficacy-toxicity window of ADCs in clinical development, this insight is also valuable for dose selection to maintain a balance of safety and efficacy of ADCs.

6. Conclusion

A population PK/PD model was built to establish concentration-effect relationship of ADC in preclinical model and translate its efficacy to human. Efficacy predicted using clinically relevant population PK/PD model showed remarkable PFS in both Q1W and Q3W dosing regimen in the dose range of 0.5 to 2 mg/kg or 1.3 to 3.9 mg/kg. Above studies and evaluations helped us establish robust PK/PD relationship of our ADC and understand impact of maintaining steady state concentration in a certain range on the therapeutic outcome. It is evident from our findings that human dose which maintains average steady state concentrations at predicted TSC is sufficient to obtain clinical efficacy and therefore maintaining steady state trough concentrations above TSC may not be desired. Overall, 0.5 mg/kg Q1W or 1.3 mg/kg Q3W were considered to be efficacious starting dose for FIH study of our ADC.

References

1. Kamath, A. V., & Iyer, S. (2016). Challenges and advances in the assessment of the disposition of antibody-drug conjugates. *Biopharmaceutics & drug disposition, 37*(2), 66-74.
2. Mullard, A. (2015). 2014 FDA drug approvals: the FDA approved 41 new therapeutics in 2014, but the bumper year fell short of the commercial power of the drugs approved in 2013. *Nature Reviews Drug Discovery, 14*(2), 77-82.
3. Mullard 2019 FDA drug approvals. *Nature Reviews Drug Discovery 19* (2020) 79-84.
4. Khera, E., & Thurber, G. M. (2018). Pharmacokinetic and immunological considerations for expanding the therapeutic window of next-generation antibody–drug conjugates. *BioDrugs, 32*(5), 465-480.
5. Coats, S., Williams, M., Kebble, B., Dixit, R., Tseng, L., Yao, N. S., ... & Soria, J. C. (2019). Antibody–drug conjugates: future directions in clinical and translational strategies to improve the therapeutic index. *Clinical Cancer Research, 25*(18), 5441-5448.
6. Gibbs, J. P. (2010). Prediction of exposure–response relationships to support first-in-human study design. *The AAPS journal, 12,* 750-758.
7. Zhou, Q., & Gallo, J. M. (2011). The pharmacokinetic/pharmacodynamic pipeline: translating anticancer drug pharmacology to the clinic. *The AAPS journal, 13*, 111-120.
8. Agoram, B. M., Martin, S. W., & Van der Graaf, P. H. (2007). The role of mechanism-based pharmacokinetic–

pharmacodynamic (PK–PD) modelling in translational research of biologics. *Drug discovery today, 12*(23-24), 1018-1024.
9. Wong, H., Vernillet, L., Peterson, A., Ware, J. A., Lee, L., Martini, J. F., ... & Prescott, J. (2012). Bridging the gap between preclinical and clinical studies using pharmacokinetic–pharmacodynamic modeling: an analysis of GDC-0973, a MEK inhibitor. *Clinical Cancer Research, 18*(11), 3090-3099.
10. Chien, J. Y., Friedrich, S., Heathman, M. A., de Alwis, D. P., & Sinha, V. (2005). Pharmacokinetics/pharmacodynamics and the stages of drug development: role of modeling and simulation. *The AAPS journal, 7*, E544-E559.
11. Xiang, H., Bender, B. C., Reyes, A. E., Merchant, M., Jumbe, N. L. S., Romero, M., ... & Damico-Beyer, L. A. (2013). Onartuzumab (MetMAb): using nonclinical pharmacokinetic and concentration–effect data to support clinical development. *Clinical Cancer Research, 19*(18), 5068-5078.
12. Dirks, N. L., & Meibohm, B. (2010). Population pharmacokinetics of therapeutic monoclonal antibodies. *Clinical pharmacokinetics, 49*, 633-659.
13. Lucas, A. T., Robinson, R., Schorzman, A. N., Piscitelli, J. A., Razo, J. F., & Zamboni, W. C. (2019). Pharmacologic considerations in the disposition of antibodies and antibody-drug conjugates in preclinical models and in patients. *Antibodies, 8*(1), 3.
14. Li, C., Zhang, C., Deng, R., Leipold, D., Li, D., Latifi, B., ... & Kamath, A. V. (2019). Prediction of human pharmacokinetics of antibody–drug conjugates from nonclinical data. *Clinical and translational science, 12*(5), 534-544.
15. Jumbe, N. L., Xin, Y., Leipold, D. D., Crocker, L., Dugger, D., Mai, E., ... & Tibbitts, J. (2010). Modeling the efficacy of trastuzumab-DM1, an antibody drug conjugate, in mice. *Journal of pharmacokinetics and pharmacodynamics, 37,* 221-242.
16. Dedrick, R. L. (1973). Animal scale-up. *Journal of pharmacokinetics and biopharmaceutics, 1,* 435-461.
17. Dong, J. Q., Salinger, D. H., Endres, C. J., Gibbs, J. P., Hsu, C. P., Stouch, B. J., ... & Gibbs, M. (2011). Quantitative prediction of human pharmacokinetics for monoclonal antibodies: retrospective analysis of monkey as a single species for first-in-human prediction. *Clinical pharmacokinetics, 50,* 131-142.
18. Deng, R., Iyer, S., Theil, F. P., Mortensen, D. L., Fielder, P. J., & Prabhu, S. (2011, January). Projecting human pharmacokinetics of therapeutic antibodies from nonclinical data: what have we learned?. In *MAbs* (Vol. 3, No. 1, pp. 61-66). Taylor & Francis.
19. Hasegawa, M., Sone, S., Takashima, S., Li, F., Yang, Z. G., Maruyama, Y., & Watanabe, T. (2000). Growth rate of small lung cancers detected on mass CT screening. *The British journal of radiology, 73*(876), 1252-1259.
20. Wilson, D. O., Ryan, A., Fuhrman, C., Schuchert, M., Shapiro, S., Siegfried, J. M., & Weissfeld, J. (2012). Doubling times and CT screen–detected lung cancers in the Pittsburgh Lung Screening Study. *American journal of respiratory and critical care medicine, 185*(1), 85-89.
21. Coche, E. (2016). Evaluation of lung tumor response to therapy: current and emerging techniques. *Diagnostic and interventional imaging, 97*(10), 1053-1065.
22. Hwang, K. E., & Kim, H. R. (2017). Response evaluation of chemotherapy for lung cancer. *Tuberculosis and respiratory diseases, 80*(2), 136.
23. Wada, R., Erickson, H. K., Lewis Phillips, G. D., Provenzano, C. A., Leipold, D. D., Mai, E., ... & Tibbitts, J. (2014). Mechanistic pharmacokinetic/pharmacodynamic modeling of in vivo tumor uptake, catabolism, and tumor response of trastuzumab maytansinoid conjugates. *Cancer chemotherapy and pharmacology, 74*, 969-980.
24. Simeoni, M., Magni, P., Cammia, C., De Nicolao, G., Croci, V., Pesenti, E., ... & Rocchetti, M. (2004). Predictive pharmacokinetic-pharmacodynamic modeling of tumor growth kinetics in xenograft models after administration of anticancer agents. *Cancer research, 64*(3), 1094-1101.
25. Shah, D. K., Haddish-Berhane, N., & Betts, A. (2012). Bench to bedside translation of antibody drug conjugates using a multiscale mechanistic PK/PD model: a case study with brentuximab-vedotin. *Journal of pharmacokinetics and pharmacodynamics, 39,* 643-659.
26. Betts, A. M., Haddish-Berhane, N., Tolsma, J., Jasper, P., King, L. E., Sun, Y., ... & Johnson, T. R. (2016). Preclinical to clinical translation of antibody-drug conjugates using PK/PD modeling: a retrospective analysis of inotuzumab ozogamicin. *The AAPS journal, 18*, 1101-1116.
27. Singh, A. P., & Shah, D. K. (2017). Application of a PK-PD modeling and simulation-based strategy for clinical translation of antibody-drug conjugates: a case study with trastuzumab emtansine (T-DM1). *The AAPS journal, 19,* 1054-1070.
28. Wang, J., Song, P., Schrieber, S., Liu, Q., Xu, Q., Blumenthal, G., ... & Rahman, A. (2014). Exposure–response relationship of T-DM1: insight into dose optimization for patients with HER2-positive metastatic breast cancer. *Clinical Pharmacology & Therapeutics, 95*(5), 558-564.